SIAM J. APPL. MATH.
Vol. 72, No. 2, pp. 489–511

STABILITY OF MULTICOMPONENT BIOLOGICAL MEMBRANES*

SEFI GIVLI†, HA GIANG‡, AND KAUSHIK BHATTACHARYA‡

Abstract. Equilibrium equations and stability conditions are derived for a general class of multicomponent biological membranes. The analysis is based on a generalized Helfrich energy that accounts for geometry through the stretch and curvature, the composition, and the interaction between geometry and composition. The use of nonclassical differential operators and related integral theorems in conjunction with appropriate composition and mass conserving variations simplify the derivations. We show that instabilities of multicomponent membranes are significantly different from those in single component membranes, as well as those in systems undergoing spinodal decomposition in flat spaces. This is due to the intricate coupling between composition and shape as well as the nonuniform tension in the membrane. Specifically, critical modes have high frequencies unlike single component vesicles and stability depends on system size unlike in systems undergoing spinodal decomposition in flat space. An important implication is that small perturbations may nucleate localized but very large deformations. We show that the predictions of the analysis are in qualitative agreement with experimental observations.

Key words. stability, membrane, biological, spherical, heterogeneous

AMS subject classifications. 74K25, 92C05, 49Q10

DOI. 10.1137/110831301

1. Introduction.

Biological membranes (BMs) are fundamental building blocks of cell walls, mitochondria, and other organelles. They protect the cell by providing a barrier, and control almost all interaction with the surroundings, including transport, signaling, transduction, and adhesion. A key to this diverse functionality is the coupling between mechanical signals carried by the BM and biochemical events in the cell [13, 24, 31, 37, 47] and the rich phenomena that this coupling creates; see, e.g., [3, 16, 34, 28, 36]. For example, gated mechano-sensitive ion channels open to form a large conductance pore in response to membrane stretching [14, 17, 18, 33, 38, 25].

BMs are primarily made of a lipid bilayer, but also contain proteins, rigid cholesterol molecules, and other functional molecules [9]. Moreover, for the same lipid, various phases may be found, such as gels, liquid disordered phases, and liquid ordered phases. These phases differ in their mechanical properties, which makes the BM a heterogeneous mechanical structure. Moreover, BMs are dynamic structures whose molecular arrangements can change with conditions. Depending on the type of lipids and the functional molecules involved, as well as the external conditions like osmotic pressure and temperature, the BM can remain homogeneous or segregate into different phases/domains. The latter changes the stress distribution in the BM and either absorbs or releases energy. Therefore, just like other heterogeneous materials, deformation of the BM is dictated by composition. However, unlike standard mechanical structures, composition is modulated by the shape of the BM [26].

*Received by the editors April 18, 2011; accepted for publication (in revised form) December 28, 2011; published electronically March 1, 2012. This work was supported by the U.S. National Science Foundation (DMS060667).

http://www.siam.org/journals/siap/72-2/83130.html

†Faculty of Mechanical Engineering, Technion – Israel Institute of Technology, Haifa 32000, Israel (givli@technion.ac.il).

‡Division of Engineering and Applied Science, California Institute of Technology, Pasadena, CA 91125 (hagiang@caltech.edu, bhatta@caltech.edu).

The inherent coupling between the shape and composition of the BM is an important avenue through which cells sense their environment, and is a key mechanism for mechano-transduction in cells and other organelles. For example, proteins that act on the membrane like wedges lead to areas with high curvature. In addition, certain types of functional proteins concentrate in domains of curvature that they prefer, leading to the formation of functionalized domains [30, 29]. The formation of such domains controls membrane transport as well as cellular sensing and signaling.

While the mechanics of BMs has been studied theoretically extensively [27, 46, 10] since the pioneering work of Helfrich [12], much of it focuses on single component (homogeneous) membranes. Work on multicomponent BMs either relies on advanced numerical methods such as nonlinear finite elements and phase field methods [21, 7, 20, 11, 8], or uses models with various simplifying assumptions such as axi-symmetry, small deformations, spherical caps landscape, and complete separation of the phases [2, 15, 35, 5]. Nevertheless, the literature still lacks a systematic derivation of equilibrium equations along with stability conditions for the general class of heterogeneous BMs.

In this work we systematically derive the equilibrium equations and (linear) stability conditions for a general class of multicomponent BMs motivated by the following facts: (i) stable configurations are the observable in most experiments; (ii) chemomechanical instabilities in cell membranes often relate to critical changes in biochemical processes, cell behavior, or fate. Examples are formation of focal adhesions, initiation of filopodia, and opening of ion channels; (iii) knowledge of the stability conditions can be used to measure, indirectly, mechanical and chemical properties of lipids, protein aggregates, and other functional components of the membrane.

We consider a closed BM composed of two phases. These can represent two different lipid phases (e.g., liquid ordered and liquid disordered phases), two different types of lipid molecules, or mobile membrane proteins embedded in a lipid phase. Equilibrium equations and stability conditions are obtained by calculating the first and second variations of a generalized Helfrich energy functional. We assume that overall composition, i.e., the total number of molecules of each phase, does not change in the course of the experiment. In calculating the variations of the energy functional we take advantage of nonclassical differential operators and related integral theorems developed by Yin and collaborators [42, 40, 41, 44, 39, 43]. Further, we introduce density and composition conserving variations, so that the use of Lagrange multipliers is avoided. In addition we account for the spatial nonuniform stretching of the membrane. This feature, which is commonly ignored by assuming a constant membrane area, is especially important in multicomponent membrane applications, and can have important implications in processes such as the activity of gated ion channels.

The manuscript is arranged as follows. Our model is introduced in section 2. Section 3 provides some mathematical preliminaries including the operators and identities that enable this calculation and the form of the perturbations. Calculation of the first variation and corresponding equilibrium equations are detailed in section 4. Stability conditions are derived in section 5. Section 6 specializes to a uniform spherical membrane and provides a detailed analysis of the stability. Main conclusions are discussed in section 7.

2. A model of a multicomponent vesicle.

2.1. The energy functional. We consider a closed lipid membrane composed of two components, which we shall refer to as type I and type II. These can represent two different lipid phases (e.g., liquid ordered and liquid disordered phases), two different

types of lipid molecules, or mobile membrane proteins embedded in a lipid phase. The current geometric configuration of the membrane is described by a closed surface S. Let H be the mean curvature, let K be the Gauss curvature of this surface, and let V_S be the volume enclosed by S. We introduce a total density $\rho : S \to R^+$ that describes the total density (both components combined) at each point of the membrane, and a concentration $c : S \to [0, 1]$ which describes the ratio between the two components. It follows that at any given point on the membrane $c\rho$ and $(1 - c)\rho$ are the densities of component I and component II, respectively. Further, if M_{I} and M_{II} denote the total number of molecules of each component, we have

$$\int_S c\rho \, dS = M_{\mathrm{I}} \quad \text{and} \quad \int_S \rho \, dS = M \qquad (M \equiv M_{\mathrm{I}} + M_{\mathrm{II}}). \tag{1}$$

Suppose that this membrane is subjected to an osmotic pressure difference P between the fluid inside and outside the vesicle. Then, the total potential energy of the vesicle may be written as

$$\mathcal{F} = \int_S \phi(H, K, \rho, c) \, dS - P V_S, \tag{2}$$

where the generalized free energy is given by

$$\phi(H, K, \rho, c) = k_\rho \left(\frac{\rho}{\rho_0} - 1 \right)^2 + \frac{1}{2} k_H(c) \left(2H - H_0(c)\right)^2 + k_K K + f(c) + \frac{1}{2} k_c |\nabla c|^2. \tag{3}$$

The first term depends on the density or equivalently the specific area, and describes the energy required to stretch the membrane. Therefore we refer to k_ρ as the stretching modulus. Importantly, this term depends only on specific area instead on the entire metric tensor. This reflects the fact that the membrane is a fluid and cannot resist any shear in the plane. Various researchers use the fact that k_ρ is large and replace this energy with a constraint of constant membrane area [27, 46]. While this is acceptable for single component BMs, it makes certain subtleties harder in multicomponent situations which we shall see later.

The second term is the Helfrich energy and depends on the mean curvature. k_H is the bending modulus and H_0 is the spontaneous curvature, and both depend on composition. If the two components have different molecular structure, any inhomogeneity induces a local spontaneous curvature. Therefore, spontaneous curvature is dictated by composition, resulting in a coupling between composition and shape. For example, membrane proteins can act on the membrane as wedges leading to areas of high curvature. Also, different types of lipids can have different molecular shapes. For example, in phosphatidylcholine the head group and lipid backbone have similar cross-sectional areas, and therefore the molecule has a cylindrical shape. On the other hand, phosphatidylethanolamine molecules have a small headgroup and are cone-shaped, while in lysophosphatidylcholine the hydrophobic part occupies a relatively smaller surface area and the molecule has the shape of an inverted cone [30]. The mixture of cylindrical lipids and conical lipids will have a spontaneous curvature that depends on the concentration of the conical lipids [6]. In addition, the two phases can have different mechanical properties. This is accounted for by the dependency of k_H on composition [3].

The third term is taken to be linear in the Gauss curvature and, consequently, does not affect closed vesicles.

The fourth term, f, describes the interaction between the two phases. A simple model for f combines the aggregation enthalpy and the entropy of mixing [35]

$$f = k_B T \rho_0 \left(c \ln c + (1-c)\ln(1-c)\right) + \frac{1}{2} B \rho_0 c(1-c) \tag{4}$$

so that it is convex at high temperatures (miscible) but nonconvex at low temperatures (immiscible). This above form is similar to relations used in other works [1, 19], where fourth-order polynomials have been used in order to approximate a double-well energy landscape. It turns out that the critical temperature, $B/4k_B$, is typically close to room temperature [35].

Finally, the last term penalizes rapid changes in composition as, for example, in phase boundaries.

2.2. Nondimensionalization. We define the unit length R as the radius of the membrane if it takes a spherical shape with a uniform density $\rho = \rho_0$. Hence,

$$M = 4\pi R^2 \rho_0. \tag{5}$$

Accordingly, we introduce the following nondimensional quantities:

$$\widetilde{H} = HR, \quad \widetilde{K} = KR^2, \quad \widetilde{\nabla} = R\nabla, \quad \widetilde{\rho} = \frac{\rho}{\rho_0}, \quad \widetilde{P} = \frac{P}{k_H^*} R^3, \tag{6}$$

and

$$\widetilde{k}_H = \frac{k_H}{k_H^*}, \quad \widetilde{k}_K = \frac{k_K}{k_H^*}, \quad \widetilde{k}_\rho = \frac{k_\rho}{k_H^*} R^2, \quad \widetilde{k}_c = \frac{k_c}{k_H^*}, \tag{7}$$

where $k_H^* = k_H\,|_{c=0.5}$. Therefore, the nondimensional energy functional reads as

$$\widetilde{F} = \frac{F}{k_H^*} = \int_{\widetilde{S}} \widetilde{\phi}\, d\widetilde{S} - \widetilde{P}\widetilde{V}_S, \tag{8}$$

where

$$\begin{aligned} \widetilde{\phi}(\widetilde{H}, \widetilde{K}, \widetilde{\rho}, \widetilde{c}) &= \frac{R^2}{k_H^*}\phi \\ &= \widetilde{k}_\rho \left(\widetilde{\rho} - 1\right)^2 + \frac{1}{2}\widetilde{k}_H \left(2\widetilde{H} - \widetilde{H}_0(c)\right)^2 \\ &\quad + \widetilde{k}_K \widetilde{K} + \widetilde{f}(c) + \frac{1}{2}\widetilde{k}_c |\widetilde{\nabla} c|^2. \end{aligned} \tag{9}$$

In what follows all quantities are nondimensional, and we disregard the ($\sim$) symbol for brevity.

3. Mathematical preliminaries.

3.1. Definitions and identities. We have represented a biological membrane as a surface or a two-dimensional manifold in a three-dimensional Euclidean space. This surface is described by

$$\mathbf{x} = \mathbf{x}(u^i), \quad i = 1, 2,$$

where u^1, u^2 are real parameters. We introduce the following quantities:

$$\begin{aligned}
&\mathbf{g}_i = \mathbf{x}_{,i}, && g_{ij} = \mathbf{g}_i \cdot \mathbf{g}_j, \quad && g = \det(g_{ij}),\\
&\mathbf{g}^i \cdot \mathbf{g_j} = \delta_{ij}, && g^{ij} = (g_{ij})^{-1}, &&\\
&\mathbf{n} = g^{-1/2}(\mathbf{g_1} \times \mathbf{g_2}), && L_{ij} = \mathbf{g}_{i,j} \cdot \mathbf{n}, \quad && L = \det(L_{ij}).
\end{aligned}$$

Here, $(.)_{,i}$ denotes partial derivative with respect to u^i, $\mathbf{g}_i$ and $\mathbf{g}^i$ are, respectively, the covariant and contravariant base vectors tangent to the surface, $\mathbf{n}$ is the unit normal to the surface, δ_{ij} is the Kronecker delta, and g_{ij} and L_{ij} are the first and second fundamental forms of the surface. In addition, the mean and Gauss curvatures of the surface are

$$H = \frac{1}{2}(c_1 + c_2) = \frac{1}{2} g^{ij} L_{ij}, \quad K = c_1 c_2 = \frac{L}{g},$$

where c_1 and c_2 are the principle normal curvatures.

The surface gradient operator is defined as [32]

$$\nabla = \mathbf{g}^i \frac{\partial}{\partial u^i}.$$

Accordingly, the gradient of a scalar function f is simply

$$\nabla f = \mathbf{g}^i \frac{\partial}{\partial u^i} = f_{,j} \mathbf{g}^j,$$

and the Laplace–Beltrami operator is

$$\Delta f = \nabla^2 f \equiv \nabla \cdot \nabla f = \frac{1}{\sqrt{g}} \left(\sqrt{g} f_{,i} g^{ij} \right)_{,j}.$$

We recall two integral identities:

$$\int_S \nabla f \, dS = -\int_S 2\, H\, f\, \mathbf{n} \, dS, \quad \int_S \nabla \cdot \mathbf{v} \, dS = -\int_S 2\, H\, \mathbf{v} \cdot \mathbf{n} \, dS. \tag{10}$$

In addition to the above conventional surface operators, we shall also use extensively the following nonconventional operators introduced by Yin and his collaborators[1] [23, 41]:

$$\overline{\nabla} = K \overline{L}^{ij} \mathbf{g}_i \frac{\partial}{\partial u^j}, \quad L_{im} \overline{L}^{mj} = \delta_{ij}; \tag{11}$$

$$\overline{\nabla}^2 f \equiv \nabla \cdot \overline{\nabla} f = \overline{\nabla} \cdot \nabla f = \frac{1}{\sqrt{g}} \left(\sqrt{g} K \overline{L}^{ij} f_{,i} \right)_{,j}. \tag{12}$$

These operators satisfy a number of integral identities that will prove useful in our calculations. These are listed in Appendix A. They largely follow from the following identities, which appear to be formal analogues of (10) with the Gauss curvature replacing by mean curvature:

$$\int_S \overline{\nabla} f \, dS = -\int_S 2\, K\, f\, \mathbf{n} \, dS, \quad \int_S \overline{\nabla} \cdot \mathbf{v} \, dS = -\int_S 2\, K\, \mathbf{v} \cdot \mathbf{n} \, dS. \tag{13}$$

[1] Yin refers to them as the second gradient and second divergence operators, but we do not use that terminology here.

3.2. Perturbations. We are interested in finding the equilibria and study their stability by studying the first and second variation of the potential energy. This requires some care since the perturbations in shape, density, and composition can be coupled and because of the constraints (1). Consider arbitrary perturbations of shape, density, and composition:

$$\mathbf{x}' = \mathbf{x} + \delta\mathbf{x}, \quad \rho' = \rho + \delta\rho, \quad c' = c + \delta c, \tag{14}$$

where

$$\delta\mathbf{x} = \mathbf{n}\,(\epsilon\,\zeta_1 + \epsilon^2\zeta_2), \quad \delta\rho = \epsilon\,\zeta_3 + \epsilon^2\zeta_4, \quad \delta c = \epsilon\,\zeta_5 + \epsilon^2\zeta_6, \tag{15}$$

ζ_i are arbitrary functions, and ϵ is an arbitrarily small scalar. The fact that we are dealing with a closed smooth surface enables us to use normal perturbations without any loss of generality. To deal with the constraints (1), we introduce

$$G_1(\rho, S) = \int_S \rho\, dS \qquad \text{and} \qquad G_2(\rho, c, S) = \int_S \rho\, c\, dS. \tag{16}$$

Evaluating these for the perturbed quantity and expanding them in ϵ, we obtain

$$\begin{aligned}
G_1(\rho', S') =& G_1(\rho, S) + \epsilon \int_S \{\zeta_3 - 2H\rho\zeta_1\}\, dS \\
&+ \epsilon^2 \int_S \left\{ K\rho\zeta_1^2 - 2H\zeta_1\zeta_3 + \zeta_4 - 2H\zeta_2\rho + \frac{1}{2}\rho\,|\nabla\zeta_1|^2 \right\} dS \\
&+ \mathcal{O}(\epsilon^3), \\
G_2(\rho', c', S',) =& G_2(\rho, c, S) + \epsilon \int_S \big\{ c[\zeta_3 - 2H\rho\zeta_1] + \rho\zeta_5 \big\} dS \\
&+ \epsilon^2 \int_S \left\{ c\left[K\rho\zeta_1^2 - 2H\zeta_1\zeta_3 + \frac{1}{2}\rho\,|\nabla\zeta_1|^2 \right] + \zeta_5[\zeta_3 - 2H\rho\zeta_1] \right. \\
&\qquad \left. - 2cH\zeta_2\rho + c\zeta_4 + \zeta_6\rho \right\} dS + \mathcal{O}(\epsilon^3).
\end{aligned} \tag{17}$$

In order for the constraints to satisfy up to the second order, we need

$$\begin{aligned}
&\int_S \{\zeta_3 - 2H\rho\zeta_1\}\, dS = 0, \\
&\int_S \left\{ K\rho\zeta_1^2 - 2H\zeta_1\zeta_3 + \zeta_4 - 2H\zeta_2\rho + \frac{1}{2}\rho\,|\nabla\zeta_1|^2 \right\} dS = 0, \\
&\int_S \big\{ c[\zeta_3 - 2H\rho\zeta_1] + \rho\zeta_5 \big\} dS = 0, \\
&\int_S \left\{ c\left[K\rho\zeta_1^2 - 2H\zeta_1\zeta_3 + \frac{1}{2}\rho\,|\nabla\zeta_1|^2 \right] \right. \\
&\qquad \left. + \zeta_5[\zeta_3 - 2H\rho\zeta_1] - 2cH\zeta_2\rho + c\zeta_4 + \zeta_6\rho \right\} dS = 0.
\end{aligned} \tag{18}$$

It follows that there exist functions $\beta_1, \beta_2, \gamma_1, \gamma_2$ such that

(19)
$$\begin{aligned}
\Delta\gamma_1 &= \zeta_3 - 2H\rho\zeta_1,\\
\Delta\gamma_2 &= K\rho\zeta_1^2 - 2H\zeta_1\zeta_3 + \zeta_4 - 2H\zeta_2\rho + \frac{1}{2}\rho\left|\nabla\zeta_1\right|^2,\\
\Delta\beta_1 &= c[\zeta_3 - 2H\rho\zeta_1] + \rho\zeta_5,\\
\Delta\beta_2 &= c\left[K\rho\zeta_1^2 - 2H\zeta_1\zeta_3 + \frac{1}{2}\rho\left|\nabla\zeta_1\right|^2\right] + \zeta_5[\zeta_3 - 2H\rho\zeta_1] - 2cH\zeta_2\rho + c\zeta_4 + \zeta_6\rho.
\end{aligned}$$

Solving (19) for $\zeta_{i,\, i=\overline{3,6}}$ and substituting them into (15) we have

(20)
$$\begin{aligned}
\delta\rho &= \epsilon\left\{2H\rho\zeta_1 + \Delta\gamma_1\right\}\\
&\quad + \epsilon^2\left\{2H\rho\zeta_2 + \zeta_1^2[4H^2 - K]\rho - \frac{1}{2}\rho|\nabla\zeta_1|^2 + 2H\zeta_1\Delta\gamma_1 + \Delta\gamma_2\right\},\\
\delta c &= \epsilon\frac{\Delta\beta_1 - c\Delta\gamma_1}{\rho} + \epsilon^2\frac{\rho\Delta\beta_2 - \Delta\beta_1\Delta\gamma_1 + c(\Delta\gamma_1)^2 - c\rho\Delta\gamma_2}{\rho^2}.
\end{aligned}$$

We have shown that any arbitrary perturbation that satisfies the constraint to second order is necessarily of the form (20). The converse is also true by verification. Note also that $\zeta_i, \beta_i, \gamma_i, i = 1, 2$, are independent.

Finally, we note that in light of the specific form of (20), taking first and second variations with respect to ζ_2, β_2, and γ_2 does not yield any new information. Thus, we take the variation of the surface, density, and composition to be

(21)
$$\begin{aligned}
\delta\mathbf{x} &= \epsilon\psi_1\mathbf{n},\\
\delta\rho &= \epsilon\left(2H\rho\psi_1 + \Delta\psi_2\right)\\
&\quad - \epsilon^2\left((K - 4H^2)\rho\psi_1^2 + \frac{1}{2}\rho|\nabla\psi_1|^2 - 2H\psi_1\Delta\psi_2\right),\\
\delta c &= \epsilon\frac{\Delta\psi_3 - c\Delta\psi_2}{\rho} - \epsilon^2\Delta\psi_2\frac{\Delta\psi_3 - c\Delta\psi_2}{\rho^2}
\end{aligned}$$

for arbitrary functions $\psi_i, i = 1, 2, 3$. Another way to approach the problem is to introduce Lagrange multipliers associated with the constraints (1). Details on the equivalence between the two approaches are provided in Appendix C.

4. Equilibrium configurations. We now derive the equilibrium equations in accordance with section 3.2. By definition,

(22)
$$\delta^{(1)}\mathcal{F} = \left.\frac{d\mathcal{F}(\mathbf{x} + \delta\mathbf{x}, \rho + \delta\rho, c + \delta c)}{d\epsilon}\right|_{\epsilon=0}.$$

Plugging (21) into (22), applying integral theorems associated with the conventional and nonconventional gradient operators, and letting $\delta^{(1)}\mathcal{F} = 0$ for arbitrary ψ_i, we conclude, after some algebraic manipulations, with the following three equilibrium equations:

(23a)
$$\begin{aligned}
&\Delta(k_H(c)(2H - H_0(c))) + 4k_H(c)H(H^2 - K) + k_H(c)H_0(c)(2K - HH_0(c))\\
&\qquad - 2Hf(c) + k_c(H|\nabla c|^2 - \nabla c\cdot\widetilde{\nabla}c) + 2k_\rho H(\rho^2 - 1) - P = 0,
\end{aligned}$$

$$\Delta\left(2k_\rho(\rho-1)+c\frac{k_H(c)H_0^{'}(c)(2H-H_0(c))-f^{'}(c)+k_c\Delta c}{\rho}\right.$$
$$\left.-\frac{c\,k_H^{'}(c)(2H-H_0(c))^2}{2\rho}\right)=0, \tag{23b}$$

$$\Delta\left(-\frac{k_H(c)H_0^{'}(c)(2H-H_0(c))-f^{'}(c)+k_c\Delta c}{\rho}+\frac{k_H^{'}(c)(2H-H_0(c))^2}{2\rho}\right)=0, \tag{23c}$$

where $()^{'}$ denotes the derivative with respect to c.

Equation (23a) is associated with variations in the membrane shape, and generalizes the *shape equation* for single component membranes [46]. The first three terms, which include the coefficient k_H, describe the contribution of bending. There is no term involving k_K because the integral of the Gauss curvature is conserved on a closed surface according to the Gauss–Bonnet theorem. The fourth and fifth terms come from the free energy associated with composition. The final two terms are a generalization of the Young–Laplace equation, and we identify $2k_\rho(\rho^2-1)$ as the membrane tension.

Similarly, we denote the equations associated with the perturbations in ρ (23b) and in c (23c) the *density* and *composition equations*, respectively. We note that if $\Delta\varphi=0$ over a closed surface, φ is a constant function:

$$\Delta\varphi=0\Rightarrow 0=\int_S\varphi\Delta\varphi\,dS=-\int_S\nabla\varphi\cdot\nabla\varphi\,dS$$
$$\Rightarrow\nabla\varphi=0\Rightarrow\varphi=\text{const.} \tag{24}$$

Therefore, we can combine the density and composition equations, and show that

$$2k_\rho(\rho^2-1)=(\rho+1)(\alpha_2+\alpha_1 c), \tag{25}$$

where α_1 and α_2 are constants. It follows that the membrane tension is not necessarily uniform in multicomponent membranes. Further, the coefficient α_1 linking tension and composition is a generalized specific chemical potential. Interestingly, this potential depends on both membrane shape and composition. Finally, the composition equation (23c) may be interpreted as a generalized Cahn–Hilliard equation. The presence of $H_0^{'}(c)$ indicates that shape can drive nontrivial variations in composition even when $f(c)$ is convex ($f^{'}(c)$ monotone).

5. Linear stability. The three coupled equations (23) enable us to find equilibrium configurations. Nevertheless, an equilibrium configuration is not necessarily a stable one. We therefore proceed with analyzing the linear stability of the equilibrium solutions by investigating the second variation of the energy functional

$$\delta^{(2)}\mathcal{F}=\left.\frac{d^2F(\mathbf{x}+\delta\mathbf{x},\rho+\delta\rho,c+\delta c)}{d\epsilon^2}\right|_{\epsilon=0} \tag{26}$$

with respect to (21). By applying integral theorems associated with the conventional and nonconventional gradients, we are able to write the second variation in the following compact form:

$$\delta^{(2)}\mathcal{F}=\int_S\sum_{i,j=1}^{3}D_{ij}\psi_i\psi_j\,dS, \tag{27}$$

where D is a symmetric differential operator with the following components:
(28)

$$
\begin{aligned}
D_{11}\psi_1\psi_1 =& k_H(c)(\Delta\psi_1)^2 - k_c(\nabla c\cdot\nabla\psi_1)^2 + 2k_H(c)(2H-H_0)(2\psi_1\nabla H\\
&- \overline{\nabla}\psi_1)\cdot\nabla\psi_1 + \{2k_\rho[K(1-\rho^2)+4H^2\rho^2] + 2k_c[|\nabla c|^2(2H^2-K)\\
&- H\nabla c\cdot\overline{\nabla}c] + K[k_H(c)(H_0^2-20H^2+4K)+2f] + 16k_H(c)H^4\\
&+ 2PH\}\psi_1^2 + \left\{\frac{1}{2}k_H(c)H_0(H_0-8H) + \frac{1}{2}k_c|\nabla c|^2 + k_\rho(1-\rho^2) + f\right.\\
&\left.+ k_H(c)6H^2\right\}|\nabla\psi_1|^2 + 4k_H(c)\{4H^2 - HH_0 - K\}\psi_1\Delta\psi_1,\\
D_{12}\psi_1\psi_2 =& \frac{c\Delta\psi_2}{\rho}\left\{2k_c\nabla c\cdot[\nabla(H\psi_1) - \overline{\nabla}\psi_1] + k_H(c)H_0^{'}\Delta\psi_1 + \left[2k_c(H\Delta c - \overline{\Delta}c)\right.\right.\\
&+ 2(Hf^{'} + k_H(c)(HH_0H_0^{'} - KH_0^{'})) + 4k_\rho H\frac{\rho^2}{c}\Big]\psi_1\\
&\left.-k_H^{'}(c)(2H-H_0(c))[\Delta\psi_1 + HH_0(c)\psi_1 + 2(H^2-K)\psi_1]\right\},\\
D_{13}\psi_1\psi_3 =& \frac{\Delta\psi_3}{\rho}\left\{2k_c\nabla c\cdot[\overline{\nabla}\psi_1 - \nabla(H\psi_1)] - k_H(c)H_0^{'}\Delta\psi_1\right.\\
&- 2[k_c(H\Delta c - \overline{\Delta}c) + Hf^{'}HH_0H_0^{'} - k_H(c)KH_0^{'}]\psi_1\\
&\left.+k_H^{'}(c)(2H-H_0(c))[\Delta\psi_1 + HH_0(c)\psi_1 + 2(H^2-K)\psi_1]\right\},\\
D_{22}\psi_2\psi_2 =& \frac{c\Delta\psi_2}{\rho}\left\{\frac{\Delta\psi_2}{\rho}[k_H(c)H_0^{'}(cH_0^{'} + 2H_0 - 4H) + 2f^{'} - 2k_c\Delta c\right.\\
&\left.+ 2k_\rho\frac{\rho^2}{c} + cQ + k_H^{'}(c)(2H - H_0(c) - 2cH_0^{'}(c))] - k_c\Delta\left(\frac{c\Delta\psi_2}{\rho}\right)\right\},\\
D_{23}\psi_2\psi_3 =& \Delta\psi_2\left\{\frac{c}{\rho}k_c\Delta\left(\frac{\Delta\psi_3}{\rho}\right) - \frac{1}{\rho^2}\left[k_H(c)H_0^{'}(cH_0^{'} + H_0 - 2H) + f^{'}\right.\right.\\
&\left.\left.- k_c\Delta c + cQ + \frac{1}{2}k_H^{'}(c)(2H-H_0(c))(2H - H_0(c) - 4cH_0^{'}(c))\right]\Delta\psi_3\right\},\\
D_{33}\psi_3\psi_3 =& \frac{\Delta\psi_3}{\rho}\left\{\frac{\Delta\psi_3}{\rho}\left[Q + k_H(c)H_0^{'2} - 2k_H^{'}(c)H_0^{'}(c)(2H - H_0(c))\right]\right.\\
&\left.- k_c\Delta\left(\frac{\Delta\psi_3}{\rho}\right)\right\},
\end{aligned}
$$

and

$$
Q = f^{''}(c) - k_H(c)H_0^{''}(c)(2H - H_0(c)) + \frac{1}{2}k_H^{''}(c)(2H - H_0(c))^2. \tag{29}
$$

Notice from (28) that D_{11} generalizes what one expects for single component vesicles [46]. Also, the important interplay between composition and geometry is captured by the parameter Q, which is the unique combination through which the second derivatives of both f and H_0 appear. It shows that instabilities may be triggered by f, or by H_0 or by size.

The critical configurations are identified by the solution of the eigenvalue problem associated with (27). Further, stability can be examined by studying the eigenvalues of the operator D. In general, achieving this is difficult even for the homogeneous

membrane [46]. Nevertheless, (27) provides a powerful tool for numerical analysis of the stability of any equilibrium configuration.

6. The uniform spherical membrane.

6.1. The uniform spherical membrane. Besides being an attractive mathematical problem, the stability of a uniform spherical membrane is of practical importance. Many experiments on multicomponent vesicles have demonstrated a complex landscape of morphologies with a spherical (or quasi-spherical) membrane shape [2, 3, 6, 34]. Moreover, the starting point of these experiments is often spherical and uniform vesicles, which respond to an external stimulation, such as changes in temperature or in osmotic pressure, by altering their composition, landscape, and shape.

Let us use standard spherical coordinates, and denote the equilibrium state associated with the uniform spherical membrane with an overbar. Thus,

$$\overline{H} = -\overline{R}^{-1}, \quad \overline{K} = \overline{H}^2, \tag{30}$$

where $\overline{R}$ is the radius of the sphere. Also, the Laplace–Beltrami operator is the usual Laplace operator on the sphere, i.e.,

$$\nabla^2 y = \Delta y = \frac{1}{R^2 \sin\theta}\left((y_{,\theta}\sin\theta)_{,\theta} + \frac{1}{\sin\theta} y_{,\phi\phi}\right). \tag{31}$$

Further, the Laplace–Beltrami operator and the operator $\overline{\nabla}^2$ defined in (12) satisfy the simple relation

$$\overline{\nabla}^2 y = \overline{H}\nabla^2 y. \tag{32}$$

Since density and composition are uniform, the density and composition equations (23b), (23c) are satisfied identically, and the shape equation (23a) becomes

$$k_H H_0(\overline{c})(2\overline{H}^2 - \overline{H}H_0(\overline{c})) + 2k_\rho \overline{H}(\overline{\rho}^2 - 1) - 2\overline{H}f(\overline{c}) - P = 0. \tag{33}$$

Recall that the total number of molecules in the vesicle, M, is fixed. Thus,

$$\overline{\rho} = \overline{H}^2. \tag{34}$$

Therefore, a two-phase vesicle with an overall concentration $\overline{c} = M_I/M$ can have an equilibrium configuration of uniform composition and spherical shape if

$$-2\overline{Hf} + k_H \overline{H}_0(2\overline{H} - \overline{HH}_0) + 2k_\rho \overline{H}(\overline{H}^4 - 1) - P = 0. \tag{35}$$

Above, $\overline{f}$ and $\overline{H}_0$ imply that these functions are evaluated at $\overline{c}$. Equation (35) provides an explicit expression for the relation between the pressure difference and the radius of the vesicle. We note that for a typical vesicle with a $100\,\mu$m diameter the (nondimensional) value of k_ρ is of the order 10^8. Further, pressure difference of 10 Pa corresponds to $P = 10^5$. Therefore, unless the pressure is much smaller than that, the contribution of the first two terms can be ignored. This radius-pressure relation is illustrated in Figure 1. Further, we note that for relatively low pressures $1 - \overline{H}^2 \ll 1$ (for example, with a pressure of 10 Pa, $1 - \overline{H}^2 \approx 10^{-4}$). Therefore, from (34), the density of the membrane is almost unchanged. This agrees with the

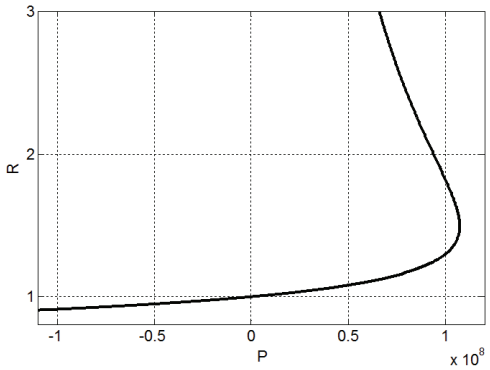

FIG. 1. *Pressure—radius relation for a uniform sphere.*

common assumption that the membrane has a constant area. Nevertheless, this assumption is questionable in cases where the (nondimensional) pressure is relatively high and the membrane is strained by a few percents, as occurs in certain cells and bacteria [4]. Importantly, the "constant area constraint" is usually imposed by introducing a constant (yet unknown) Lagrange multiplier [10, 26, 46]. Therefore, the constant area constraint implies that the membrane stretch is uniform. Obviously this is not the case in multicomponent membranes where ρ can vary considerably (25). Accounting for the nonuniform stretch is important in studying phenomena such as mechano-sensation and ion-channels activity, where membrane stretching governs the mechanical response. Our formulation accounts for the nonuniform stretch in the membrane through ρ.

Next, we calculate the second variation of the energy functional for a uniform spherical membrane. To do that, we evaluate (27) and (28) using relation (30)–(32), (34) with $\rho = \overline{\rho} = \text{const}$ and $c = \overline{c} = \text{const}$. In addition, it is convenient to expand each of the functions ψ_i into a series of spherical harmonics [46, 22]

$$\psi_i = \sum_{l,m} A_i^{(l,m)} Y^{(l,m)}, \tag{36}$$

where $A_i^{(l,m)}$ are constants and $Y^{(l,m)}$ is the spherical harmonic of degree l and order m satisfying

$$\Delta Y^{(l,m)} = -\overline{H}^2 l(l+1) Y^{(l,m)}. \tag{37}$$

Since the membrane is closed, the periodic boundary conditions, as well as regularity conditions at both the north and south poles, require that l and m be integers that satisfy

$$l \geq 0 \quad \text{and} \quad |m| \leq l. \tag{38}$$

In addition, in order to ensure that ψ_i are real functions we impose the requirement

$$\left(A_i^{(l,m)}\right)^* = (-1)^m A_i^{(l,-m)}. \tag{39}$$

Above, the asterisk refers to complex conjugate, and the relation $\left(Y^{(lm)}\right)^* = (-1)^m Y^{(l,-m)}$ has been used. With the aid of the last four equations we conclude with

$$\delta^{(2)}\mathcal{F} = \sum_{l\geq 0}\sum_{|m|\leq l} G_{ij} A_i^{(l,m)} \left(A_j^{(l,m)}\right)^*, \tag{40}$$

where G_{ij} are the components of a 3×3 symmetric matrix $\mathbf{G}$ which depends on l but not on m:

$$\begin{aligned}
G_{11} &= \overline{H}^2\Big\{k_\rho[10\overline{H}^4 - 2 + l(l+1)(1-\overline{H}^4)] \\
&\quad + \frac{1}{2}(l+2)(l-1)[\overline{k}_H(2\overline{H}^2 l(l+1) + \overline{H}_0^2 - 4\overline{HH}_0) + 2\overline{f}]\Big\}, \\
G_{12} &= \overline{H}l(l+1)\Big\{c\overline{k}_H[(\overline{H}l(l+1) + 2(\overline{H}-\overline{H}_0))\overline{H}_0^{'}] - 2c\overline{f}^{'} - 4k_\rho\overline{H}^4 \\
&\quad + \overline{k}_H^{'}\overline{c}(2\overline{H}-\overline{H}_0)(\overline{H}_0 - \overline{H}l(l+1))\Big\}, \\
G_{13} &= -\overline{H}l(l+1)\Big\{\overline{k}_H\overline{H}_0^{'}[l(l+1)\overline{H} + 2(\overline{H}-\overline{H}_0)] - 2\overline{f}^{'} \\
&\quad + \overline{k}_H^{'}(2\overline{H}-\overline{H}_0)(\overline{H}_0 - \overline{H}l(l+1))\Big\}, \\
G_{22} &= l^2(l+1)^2\Big\{2k_\rho\overline{H}^4 + k_c\overline{c}^2 l(l+1)\overline{H}^2 - \overline{c}[\overline{k}_H(4\overline{H} - 2\overline{H}_0 - \overline{c}\overline{H}_0^{'})\overline{H}_0^{'} \\
&\quad - \overline{c}\overline{Q} - 2\overline{f}^{'} + \overline{k}_H^{'}\overline{c}(2\overline{H}-\overline{H}_0)(2\overline{H}-\overline{H}_0 - 2\overline{c}\overline{H}_0^{'})]\Big\}, \\
G_{23} &= l^2(l+1)^2\Big\{l(l+1)\overline{c}\overline{H}^2 k_c + \overline{k}_H(2\overline{H} - \overline{H}_0 - \overline{c}\overline{H}_0^{'})\overline{H}_0^{'} - \overline{c}\overline{Q} - \overline{f}^{'} \\
&\quad - \frac{1}{2}\overline{k}_H^{'}(2\overline{H}-\overline{H}_0)(2\overline{H}-\overline{H}_0 - 4\overline{c}\overline{H}_0^{'})\Big\}, \\
G_{33} &= l^2(l+1)^2\Big\{l(l+1)\overline{H}^2 k_c + \overline{k}_H\overline{H}_0^{'2} + \overline{Q} - 2\overline{k}_H^{'}(2\overline{H}-\overline{H}_0)\overline{H}_0^{'}\Big\}.
\end{aligned} \tag{41}$$

The equilibrium configuration is stable if $\delta^2 F$ is positive for any $Q_i^{(l,m)}$. An equivalent representation of (40) is

$$\delta^2\mathcal{F} = \mathbf{A}\mathbf{J}\left(\mathbf{A}^*\right)^T, \tag{42}$$

where

$$\mathbf{A} = \left(\psi_1^{0,0}, \psi_2^{0,0}, \psi_3^{0,0}, \ldots, \psi_1^{l,-l}, \psi_2^{l,-l}, \psi_3^{l,-l}, \ldots, \psi_1^{l,l}, \psi_2^{l,l}, \psi_3^{l,l}\right) \tag{43}$$

and

$$\mathbf{J} = \begin{pmatrix}
[G(l=0)] & & & & & & 0 \\
& \ddots & & & & & \\
& & [G(l)] & & & & \\
& & & \ddots & & & \\
& & & & [G(l)] & & \\
& & & & & \ddots & \\
& 0 & & & & & \ddots
\end{pmatrix}. \tag{44}$$

Therefore, critical configurations can be obtained by the requirement $\det(G) = 0$, and an equilibrium configuration is stable if all three eigenvalues of $\mathbf{G}(l)$ are positive for any $l \geq 0$.

6.2. Numerical results. Equations (41) show how the stability of the uniform sphere is dictated by the mechanical properties of the membrane, k_H and k_ρ, the coupling between shape and composition, $H_0(c)$, and the nature of interaction between the two phases through $f(c)$ and k_c. While reports regarding measured values of k_H and k_ρ are consistent [4, 26], the literature still lacks systematic measurements of the other quantities. These are harder to gauge, may significantly differ for different types of lipids or proteins, and are much more sensitive to temperature. For example, the interaction function $f(c)$ may change from single well to double well energy structure by varying the temperature by a few degrees. From (4) we can calculate f'' as

$$f''|_{c=0.5} = 4\frac{R^2\rho_0}{k_H}\kappa T_0\left(\frac{T}{T_0} - \frac{B}{4\kappa T_0}\right), \tag{45}$$

where T_0 is the room temperature. Recalling that $k_H \approx 10^{-19}$ J and $\rho \approx 10^4$ molecules per μm^2 (lateral area occupied by a single membrane proteins is roughly 10 nm), we conclude that a change of one Kelvin corresponds to a change of $\sim$100 in f''. Thus, for the same composition, $f''(c)$ changes sign (from convex to concave and vice versa), which in turn can change the sign of the second variation. Therefore, in the examples below we focus on demonstrating how the stability of the uniform sphere is affected by $f''(c)$, k_c, and H_0'. Note that while changes in the first two quantities can be interpreted as changes in temperature as discussed above, H_0' reflects the strength of the coupling between composition and shape.

In all examples below we consider a 10 μm vesicle with $\overline{c} = 0.5$ ($M_I = M_{II}$). Thus, typical (dimensional) values of $k_H = 10^{-19}$ J and $k_\rho = 100\,\mathrm{mJ/m^2}$ correspond to nondimensional values of $k_H = 1$ and $k_\rho = 10^8$. In addition, we assume that $f'\big|_{\overline{c}} = 0$, which means that $\overline{c}$ locates the bottom of the composition "energy well."

Figure 2(a) illustrates a typical stability phase diagram projected on the $P - l$ plane showing stable regions (**G** positive definite) and unstable regions. A configuration is said to be stable if all modes, l, are stable. Note that a mode l describes variations in shape, composition, and density, where each of these variations is characterized by the same spherical mode l. Therefore, in what follows, we interchangeably interpret modes in terms of shape, composition, or both. We define the critical pressure P_{cr} as the lowest pressure for which the membrane is stable, and l_{cr} as the degree at P_{cr}. Figure 2(c)–(d) repeat this for different values of Q. The first observation is that in contrast to single component vesicles, multicomponent vesicles can become unstable even at high positive pressures. Second, note that the critical pressure can change dramatically with Q. As noted earlier, a few degrees Celsius change in temperature can change Q by 100s. This means that the stability can depend sensitively on temperature. Consider, for example, a membrane with $P = 1400$ (equal to 0.14 Pa which is typical and smaller than the pressure exerted by actin polymerization on the lamellipodium [35]). Such a membrane would be stable for $Q = -50$, but unstable for $Q = -100$.

A third interesting observation is that the critical modes have extremely high frequency ($l \sim 10 - 100$). This is in *marked contrast* with single component vesicles where the critical mode is always 2 [46]. However, it is completely consistent with experimental observations [3, 34]. Figure 2(b) reproduces the early stages of instability observed by Veatch and Keller [34] under two different experimental conditions. An important implication is that small perturbations may nucleate localized but very large deformations. The high frequency instability is consistent with (flat) spinodal decomposition. However, unlike (flat) spinodal decomposition, the critical temperature, pressure, and mode depend on system size through our parameter Q.

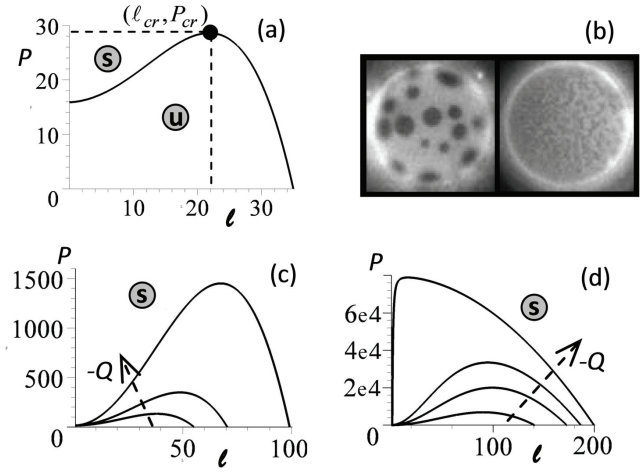

FIG. 2. *Projection of the stability phase diagram on the $P - l$ plane for different values of Q and $k_c = 0.01, H_0 = -10, H_0' = -20$. The solid line separates between stable and unstable regions, denoted here with "***s***" and "***u***," respectively.* (a) $Q = -10$, (c) $Q = -30, -50, -100$, (d) $Q = -200, -300, -3500, -400$. (b) *Immediately after temperature is lowered a characteristic length scale appears—experimental observations of* [34] *for two different setups. (Reprinted from* [34]*, Copyright* (2011)*, with permission from Elsevier.)*

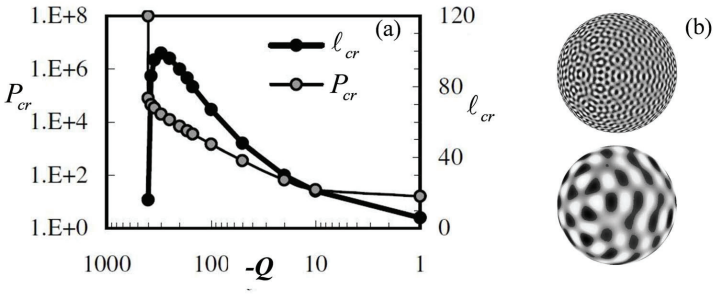

FIG. 3. (a) *Effect of temperature on critical pressure and critical mode. A change of* 100 *in Q corresponds to a few degrees Celsius. The P_{cr} curve separates between stable (above the curve) and unstable configurations ($k_c = 0.01, H_0 = -10, H_0' = -20$).* (b) *A characteristic length scale arises when a specific range of harmonics is involved. Bottom image illustrates a series of spherical harmonics with l in the range of* 14–16*, while a range of* 61–74 *on the top.*

Figure 3 plots P_{cr} and l_{cr} as functions of Q. We note a critical value for Q below which the membrane is unstable for all pressures. We also note that P_{cr} decreases monotonically with increasing Q. However, the critical mode l_{cr} is not monotonous. As Q decreases, the propensity for instability and consequently l_{cr} increases. However, increasing P_{cr} with decreasing Q increases the membrane tension. This, in turn, tries to reduce l_{cr}.

A second parameter that has a significant effect on the interplay between composition and geometry is H_0'. Figure 4 shows how critical pressure and mode depend on this parameter. We observe that the critical pressure varies nonmonotonically but

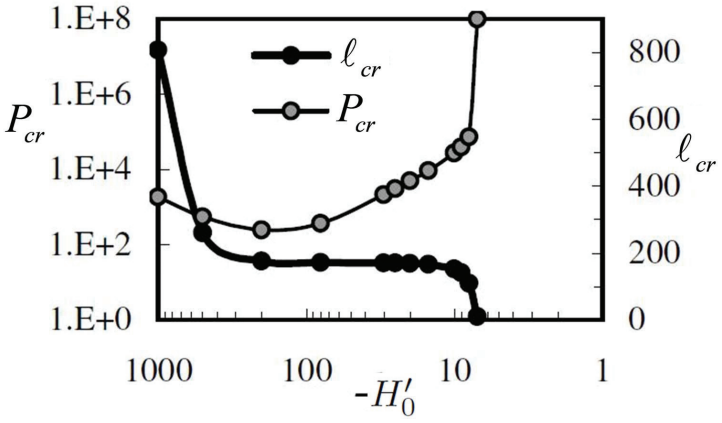

FIG. 4. *Effect of the coupling between composition and shape on critical pressure and critical mode. A negative curvature corresponds to a convex shape.*

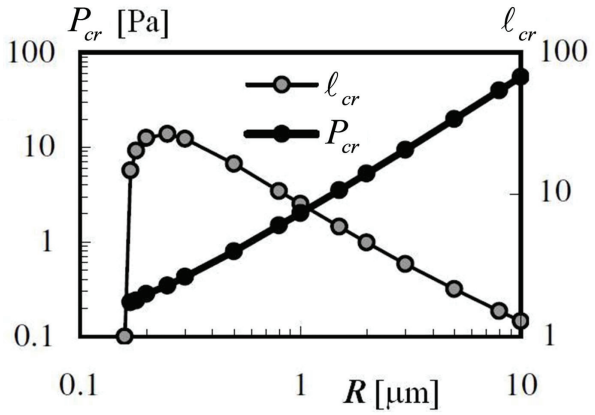

FIG. 5. *The influence of size (mass) of the vesicle on (nondimensional) critical pressure and critical mode. Nondimensional parameters are constant with values identical to Figure* 2 *with* $Q = -100$ *and* $H_0'' = -2$ *for a* $10\,\mu$m *vesicle.*

l_{cr} is monotonous. This is explained by the fact that higher values of H_0' correspond to higher spontaneous curvature of phase II, resulting in tendency of the system to have small regions in the membrane with high curvature. Interestingly, for moderate values of H_0', P_{cr} exhibits significant changes while l_{cr} is almost unaffected.

The effect of H_0', which reflects the strength of the composition-shape coupling, is demonstrated in Figure 4. Here, unlike the effect of the phase interaction discussed above, the strength of the composition-shape coupling has a nonmonotonous effect on the stability (P_{cr}) of the membrane. On the other hand, the effect on l_{cr} is monotonous. Interestingly, at moderate values of H_0', P_{cr} exhibits significant changes while l_{rc} is almost unaffected.

Figure 5 illustrates how critical pressure and mode vary with vesicle size (mass) for the same experimental setup. This is in contrast to spinodal decomposition in flat

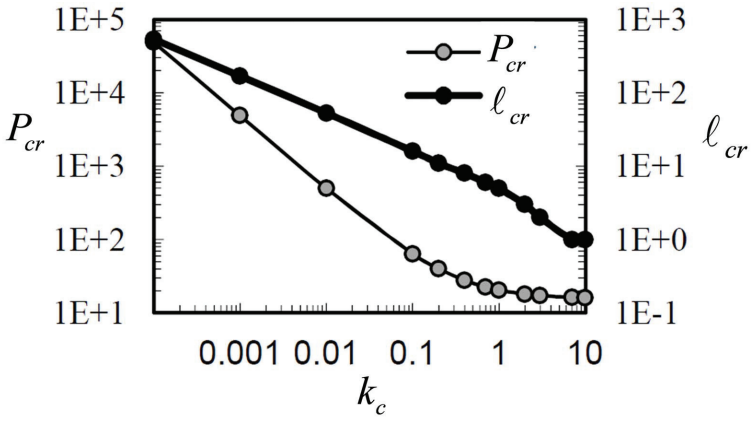

FIG. 6. *Critical pressure and critical mode as a function of* k_c.

space which is independent of mass. Note that the critical pressure tends to zero for extremely small and large systems. The former is due to the stabilizing effect of the gradient term that dominates at small sizes while the latter reflects the behavior of a flat membrane.

A higher k_c tends to make composition homogeneous. Thus, higher k_c stabilizes the membrane and excites modes with a smaller l. This is demonstrated in Figure 6 where critical pressure and mode are calculated as a function of k_c. It is evident that the effect of k_c is monotonous, and a higher k_c both stabilizes the membrane and excites modes with a smaller l. The reason is that k_c penalizes for gradients in composition. Therefore, higher values of k_c tend to stabilize the uniform composition (and in turn membrane shape as well). Furthermore, since harmonics with the same amplitude and higher l correspond to higher composition gradients, high k_c tends to diminish excitation of modes with a high l.

Finally, we demonstrate how disparity in the bending stiffness of the two components influences the membrane stability. For specificity, we assume a linear relation between the bending stiffness and composition, i.e.,

$$k_H(c) = c\,k_H^{(\mathrm{I})} + (1-c)k_H^{\mathrm{II}}, \tag{46}$$

where $k_H^{(\mathrm{I})} = k_H\big|_{c=1}$, $k_H^{(\mathrm{II})} = k_H\big|_{c=0}$ are the bending stiffness of phase I and phase II, respectively. From (41), we see that the effect of the stiffness disparity stems from (nondimensional) $k_H^{'}$. Using (46) and (7) we find that $k_H^{'} = 2\frac{r-1}{r+1}$, where $r = k_H^{(\mathrm{II})}/k_H^{(\mathrm{I})}$. Note that $|k_H^{'}|$ is bounded between zero and two. Figure 7 demonstrates how the critical pressure and critical mode are affected by the ratio $k_H^{(\mathrm{II})}/k_H^{(\mathrm{I})}$, for $H_0^{'} = -30, Q = -10, k_c = 0.01$. The asymmetric behavior with respect to $k_H^{(\mathrm{II})}/k_H^{(\mathrm{I})} = 1$ is a consequence of the spontaneous curvature.

7. Conclusions. We have derived the general form of equilibrium equations and stability conditions for multicomponent BMs. The energy functional generalizes Helfrich energy and accounts for the interaction between phases, the coupling between composition and shape, and the nonuniform spatial stretching of the membrane. The last two are specifically important in studying mechano-transduction and coupling be-

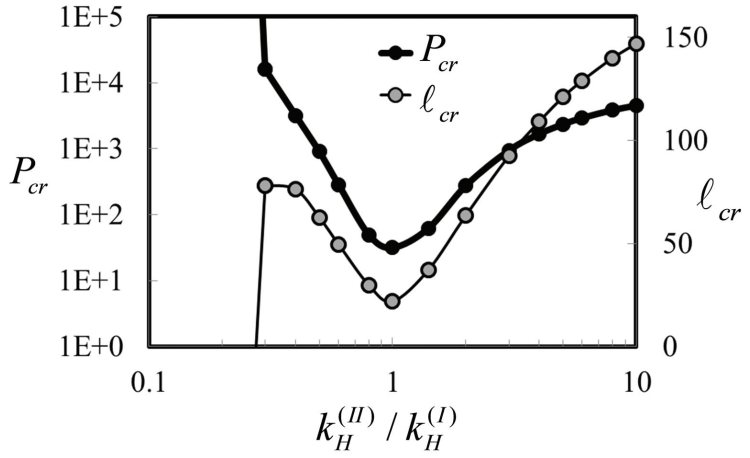

FIG. 7. *Influence of the disparity in the bending stiffness of the two components on the critical pressure and critical mode.*

tween membrane shape and biochemical events in the cell. The derivation is general and applicable to arbitrary membrane shapes, arbitrary characteristics of the interaction between the phases, and arbitrary forms of the coupling between composition and shape. Calculations of the first and second variations of the energy functional include two important features which significantly simplify the derivations and make them more elegant. These are the use of the nonconventional differential operators and related integral theorems, and the introduction of appropriate composition and mass conserving variations to avoid Lagrange multipliers.

We have practiced the stability analysis for a heterogeneous membrane with uniform composition and spherical shape. This problem is of practical importance since many experiments with multicomponent vesicles study the composition landscape of spherical (or quasi-spherical) membranes, and how uniform and spherical vesicles respond to external stimuli by altering their composition landscape and shape. We have demonstrated that the response of a heterogeneous, yet uniform, membrane is fundamentally different from that of a homogeneous (single phase) membrane. For example, single phase spherical membranes are always stable with positive pressure. Nevertheless, in the case of multicomponent membranes, chemical instabilities can drive mechanical instabilities even at relatively high pressures.

The focus of the numerical examples has been the calculation of critical pressure, under which the vesicle destabilizes, and the corresponding mode. Specifically, we performed a parametric study in order to gain insight into how the characteristics of the interaction between the phases and the strength of the coupling between composition and shape affect the membrane stability. The results are summarized in Table 1. Furthermore, we have demonstrated that the range of excited modes depends on a delicate and nonintuitive interplay between the properties of the membrane and external conditions, such as temperature and osmotic pressure. The excitation of modes with a certain range of wavelengths corresponds to a composition landscape that has a typical morphological correlation length that depends on the level of stimulation, in qualitative agreement with experimental observations.

We emphasize that our numerical results are limited to linear stability analysis,

TABLE 1
Effects of phase interaction and composition-shape coupling parameters on the stability and mode.

	Higher k_c	Higher f''	Higher H_0'
Stability	Stabilize	Stabilize	Nonmonotonous
Mode	Lower l	Nonmonotonous	Higher l

which provides important insight regarding conditions of stability and the excited modes, but does not provide information regarding the poststability behavior. This can be achieved by extending the current analysis to higher variations of the energy functional. Note that deriving these higher variations is technical in principle, as it does not require any special techniques or derivations besides the ones used for calculating the first and second variations.

Appendix A. Useful relations. In this appendix we list useful relations and identities which we have used in deriving the equilibrium equations and stability conditions. Throughout this appendix f and ψ denote arbitrary scalar functions. In addition, we consider S to be a closed surface.

The integral theorems and identities listed below are a direct consequence of the divergence theorems (10) and (13). Nevertheless, we list them here for completeness. Specifically, proofs for the identities associated with the conventional gradient operator (47)–(54) can be found in [32], while those related to the nonconventional gradient operator can be found in [42, 43]:

$$\nabla f \cdot \mathbf{n} = 0; \qquad \overline{\nabla} f \cdot \mathbf{n} = 0. \tag{47}$$

$$\nabla \cdot (\overline{\nabla} f) = \overline{\nabla} \cdot (\nabla f); \qquad \nabla f \cdot \overline{\nabla}\psi = \overline{\nabla} f \cdot \nabla\psi. \tag{48}$$

$$\int_S \nabla^2 f \, dS = 0; \qquad \int_S \overline{\nabla}^2 f \, dS = 0. \tag{49}$$

$$\int_S \nabla \cdot (f \nabla\psi) \, dS = 0; \qquad \int_S \overline{\nabla} \cdot (f \nabla\psi) \, dS = 0. \tag{50}$$

$$\int_S f \nabla^2 \psi \, dS = -\int_S \nabla f \cdot \nabla\psi \, dS; \qquad \int_S f \overline{\nabla}^2 \psi \, dS = -\int_S \nabla f \cdot \overline{\nabla}\psi \, dS. \tag{51}$$

$$\int_S (f \nabla^2 \psi - \psi \nabla^2 f) dS = 0; \qquad \int_S (f \overline{\nabla}^2 \psi - \psi \overline{\nabla}^2 f) dS = 0. \tag{52}$$

$$\nabla^2 \psi = g^{ij}(\psi_{,ij} - \Gamma^m_{ij}\psi_{,m}); \qquad \overline{\nabla}^2 \psi = K\overline{L}^{ij}(\psi_{,ij} - \Gamma^m_{ij}\psi_{,m}). \tag{53}$$

$$L_{im} g^{mn} L_{nj} = 2H L_{ij} - K g_{ij}; \qquad K\overline{L}^{ij} = 2H g^{ij} - L^{ij}. \tag{54}$$

$$|\overline{\nabla} f|^2 = -K|\nabla f|^2 + 2H \nabla f \cdot \overline{\nabla} f. \tag{55}$$

$$\overline{\nabla} f \cdot \overline{\nabla} f = 2H \nabla f \cdot \overline{\nabla} f - K \nabla f \cdot \nabla f.$$

Appendix B. Variations of various quantities. Perturbing the shape in the normal direction

$$\delta \mathbf{x} = \epsilon \psi_1 \mathbf{n}, \tag{56}$$

one can show that [46]

$$\begin{aligned}
\delta \mathbf{g}_i &= (\mathbf{n}\psi_{1,i} - L_{ij}\mathbf{g}^j\psi_1)\epsilon,\\
\delta g_{ij} &= -2L_{ij}\psi_1\epsilon + [\psi_{1,i}\psi_{1,j} + \psi_1^2 L_{im}L_{jn}g^{mn}]\epsilon^2 + \mathcal{O}(\epsilon^3),\\
\delta g &= -4gH\psi_1\epsilon + g[|\nabla\psi_1|^2 + 2\psi_1^2(2H^2+K)]\epsilon^2 + \mathcal{O}(\epsilon^3),\\
\delta g^{ij} &= 2\psi_1[2Hg^{ij} - K\overline{L}^{ij}]\epsilon + \left[\left(\frac{1}{g}e_{3i\alpha}e_{3i\beta} - g^{ij}g^{ab}\right)\psi_{1,\alpha}\psi_{1,\beta}\right.\\
&\quad \left. - 3\psi_1^2(Kg^{ij} - 4H^2g^{ij} + 2HK\overline{L}^{ij})\right]\epsilon^2 + \mathcal{O}(\epsilon^3),\\
\delta \mathbf{n} &= -\nabla\psi_1\epsilon - \left[\psi_1\psi_{1,i}L_{\alpha\beta}g^{\beta i}\mathbf{g}^\alpha + \frac{1}{2}g^{ij}\psi_{1,i}\psi_{1,j}\mathbf{n}\right]\epsilon^2 + \mathcal{O}(\epsilon^3),\\
\delta L_{\alpha\beta} &= \left[\psi_{1,\alpha\beta} - \Gamma^\gamma_{\alpha\beta}\psi_{1,\gamma} - (2HL_{\alpha\beta} - Kg_{\alpha\beta})\psi_1\right]\epsilon\\
&\quad + \left[\psi_1\psi_{1,i}\{(L_{n\alpha}g^{ni})_{,\beta} + L_{\alpha n}g^{mn}\Gamma^i_{m\beta} - L_{mn}g^{ni}\Gamma^m_{\alpha\beta}\}\right.\\
&\quad + \psi_{1,i}\psi_{1,\alpha}L_{\beta\gamma}g^\gamma g^i - \frac{1}{2}g^{ij}\psi_{1,i}\psi_{1,j}L_{\alpha\beta} + \psi_{1,\beta}\psi_{1,i}g^{ni}L_{n\alpha}\Big]\epsilon^2\\
&\quad + \mathcal{O}(\epsilon^3),
\end{aligned} \tag{57}$$

and, consequently,

$$\begin{aligned}
\delta L &= \left[\overline{\nabla}^2\psi_1 - 2HK\psi_1\right]g\epsilon + \left[\{4H^2K + 2K(K-4H^2)\}\psi_1^2\right.\\
&\quad - \frac{1}{2}K|\nabla\psi_1|^2 + K\psi_1\Delta\psi_1 - 2H\psi_1\overline{\Delta}\psi_1 - \{(L_{\alpha n}g^{ni})_{,\beta}KL^{\alpha\beta}\\
&\quad + g^{ni}KL_{mn}L^{\alpha\beta}\Gamma^m_{\alpha\beta} - g^{nm}KL_{\alpha n}L^{\alpha\beta}\Gamma^i_{m\beta}\}\psi_1\psi_{1,i}\\
&\quad \left. + e_{3\alpha\beta}(\psi_{1,1a} - \Gamma^m_{1\alpha}\psi_{1,m})(\psi_{1,2\beta} - \Gamma^n_{2\beta}\psi_{1,n})/g\right]g\epsilon^2 + \mathcal{O}(\epsilon^3),\\
\delta H &= \left[(2H^2 - K)\psi_1 + \frac{1}{2}\nabla^2\psi_1\right]\epsilon + \left[\psi_1(2H\nabla^2\psi_1 - \overline{\nabla}^2\psi_1)\right.\\
&\quad + \frac{1}{2}\nabla\psi_1\cdot(H\nabla\psi_1 - \overline{\nabla}\psi_1) + \psi_1^2H(4H^2 - 3K)\\
&\quad \left. + \psi_1\nabla H\cdot\nabla\psi_1\right]\epsilon^2 + \mathcal{O}(\epsilon^3),\\
\delta K &= \left[2HK\psi_1 + \overline{\nabla}^2\psi_1\right]\epsilon + \left[\{4H^2 - K\}K\psi_1^2 - \{(L_{\alpha n}g^{ni})_\beta\right.\\
&\quad + g^{ni}L_{mn}\Gamma^m_{\alpha\beta} - g^{mn}L_{\alpha n}\Gamma^i_{m\beta}\}KL^{\alpha\beta}\psi_1\psi_{1,i} + \frac{3}{2}K|\nabla\psi_1|^2\\
&\quad + \{K\Delta\psi_1 + 2H\overline{\Delta}\psi_1\}\psi_1\\
&\quad \left. + e_{3\alpha\beta}(\psi_{1,1a} - \Gamma^m_{1\alpha}\psi_{1,m})(\psi_{1,2\beta} - \Gamma^n_{2\beta}\psi_{1,n})/g\right]\epsilon^2 + \mathcal{O}(\epsilon^3),
\end{aligned} \tag{58}$$

$$\delta dS = -2H\psi_1 dS\,\epsilon + \left[\frac{1}{2}|\nabla\psi_1|^2 + K\psi_1^2\right]\epsilon^2 + \mathcal{O}(\epsilon^3),$$
$$\delta V_S = \epsilon\int_S \psi_1\, dS - \epsilon^2\int_S H\psi_1^2 dS + \mathcal{O}(\epsilon^3).$$

Importantly, the variation of the gradient does not equal the gradient of the variation, as in flat space. In particular, $\delta(\nabla c) \neq \nabla(\delta c)$. Also, the variation of the term in the energy function which penalizes composition gradients is

$$\begin{aligned}\delta(|\nabla c|^2) =& 2\nabla c\cdot\Big[\psi_1(H\nabla c - \overline{\nabla} c) + \nabla\Psi_3\Big]\epsilon \\ &+ \Big[|\nabla\psi_1|^2|\nabla c|^2 + 2|\nabla\Psi_3|^2 - 2(\nabla\psi_1\cdot\nabla c)^2 \\ &+ \psi_1^2(8H^2|\nabla c|^2 - 4K|\nabla c|^2 - 4H\nabla c\cdot\overline{\nabla} c) \\ &+ 8H\psi_1\nabla\Psi_3\cdot\nabla c - 8\nabla\Psi_3\cdot\overline{\nabla} c\Big]\epsilon^2 + \mathcal{O}(\epsilon^3),\end{aligned} \tag{59}$$

where $\Psi_3 = (\Delta\psi_3 - c\Delta\psi_2)/\rho$. Above, $\delta\eta$ means $\eta(\mathbf{x}+\delta\mathbf{x}) - \eta(\mathbf{x})$, and e_{ijk} is a cyclic permutation of $(1,2,3)$, i.e.,

$$e_{ijk} = \begin{cases} 1 & \text{if } (ijk) \text{ is an even permutation of (123)},\\ -1 & \text{if } (ijk) \text{ is an odd permutation of (123)},\\ 0 & \text{otherwise.}\end{cases} \tag{60}$$

Also, note the difference between L^{ij} and $\overline{L}^{ij}$: while L_{ij} and L^{ij} are the covariant and contravariant components associated with the second fundamental tensor, $\mathbf{L}$, $\overline{L}^{ij}$ are the contravariant components of $\mathbf{L}^{-1}$, i.e.,

$$L^{ij} = g^{im}g^{jn}L_{mn}; \quad L_{im}\overline{L}^{mj} = \delta_{ij}. \tag{61}$$

Appendix C. The equivalence between the tangential perturbation method and the Lagrange multiplier method. In order to solve our constrained optimization problem, the Lagrange multiplier method may be used [45]. By this method, the equilibrium solutions of (1, 3) nullify the first variation of the Lagrange functional

$$\mathcal{L} = \mathcal{F} - \lambda_1\int_S c\rho\, dS - \lambda_2\int_S \rho\, dS \tag{62}$$

with respect to any perturbations in shape, concentration, and density which take the form

$$\delta\mathbf{x} = \epsilon\psi_1\mathbf{n}, \quad \delta\rho = \epsilon\psi_2, \quad \delta c = \epsilon\psi_3. \tag{63}$$

The constants λ_1 and λ_2 in (62) are Lagrange multipliers, ψ_i in (63) are arbitrary functions, and ϵ is a small infinitesimal quantity. The equilibrium solutions are stable if the second variation is positive for any perturbations in the tangent space of the constraints:

$$\delta\mathbf{x} = \epsilon\psi_1\mathbf{n}, \quad \delta\rho = \epsilon\left(2H\rho\psi_1 + \Delta\psi_2\right), \quad \delta c = \epsilon\left(\frac{\Delta\psi_3 - c\Delta\psi_2}{\rho}\right). \tag{64}$$

Calculating the first variation of the Lagrange functional $\mathcal{L}$ under arbitrary perturbation (63) and letting it equal zero for any ψ_i, $i = \overline{1,3}$, we have the corresponding three equilibrium equations:

$$\begin{aligned}(65a)\quad &\Delta(k_H(c)(2H - H_0(c))) + 4k_H(c)H(H^2 - K) + k_H(c)H_0(c)(2K - HH_0(c))\\ &- 2Hf(c) + k_c(H|\nabla c|^2 - \nabla c \cdot \widetilde{\nabla} c) - 2H\big(k_\rho(\rho-1)^2 - \lambda_1 c\rho - \lambda_2\rho\big) - P = 0,\end{aligned}$$

$$(65b)\qquad 2k_\rho(\rho - 1) - \lambda_2 - \lambda_1 c = 0,$$

$$(65c)\qquad k_c\Delta c - f^{'}(c) + k_H(2H - H_0(c))H_0^{'}(c) + \lambda_1\rho - \frac{1}{2}k_H^{'}(c)(2H - H_0(c))^2 = 0.$$

Let's manipulate (65) and (23) to show that they are equivalent. Solving (65b) and (65c) for λ_1 and λ_2 and substituting them into (65a), we have

$$\begin{aligned}(65a\star)\quad &\Delta(k_H(c)(2H - H_0(c))) + 4k_H(c)H(H^2 - K) + k_H(c)H_0(c)(2K - HH_0(c))\\ &- 2Hf(c) + k_c(H|\nabla c|^2 - \nabla c \cdot \widetilde{\nabla} c) + 2k_\rho H(\rho^2 - 1) - P = 0,\end{aligned}$$

$$(65b\star)\qquad \lambda_2 = 2k_\rho(\rho - 1) - \lambda_1 c,$$

$$(65c\star)\qquad \lambda_1 = -\frac{k_H(2H - H_0(c))H_0^{'}(c) - f^{'}(c) + k_c\Delta c}{\rho} + \frac{1}{2\rho}k_H^{'}(c)(2H - H_0(c))^2.$$

Also, using the fact that $\Delta\varphi = 0$ on a closed surface implies that φ is a constant function, we may combine (23b) and (23c) to obtain

$$\begin{aligned}(23a\star)\quad &\Delta(k_H(2H - H_0(c))) + 4k_H H(H^2 - K) + k_H H_0(c)(2K - HH_0(c))\\ &- 2Hf(c) + k_c(H|\nabla c|^2 - \nabla c \cdot \widetilde{\nabla} c) + 2k_\rho H(\rho^2 - 1) - P = 0,\end{aligned}$$

$$(23b\star)\qquad \alpha_2 = 2k_\rho(\rho - 1) - \alpha_1 c,$$

$$(23c\star)\qquad \alpha_1 = -\frac{k_H(2H - H_0(c))H_0^{'}(c) - f^{'}(c) + k_c\Delta c}{\rho} + \frac{1}{2\rho}k_H^{'}(c)(2H - H_0(c))^2,$$

where α_1 and α_2 are constants. We can see that (65$\star$) and (23$\star$) are exactly the same. A more general proof can be found in [45].

Similarly, calculating $\delta^2\mathcal{L}$ at the tangential perturbations (64) and eliminating the Lagrange multipliers λ_1 and λ_2 by using the equilibrium equations (65) we also get

$$(66)\qquad \delta^{(2)}\mathcal{L} = \int_S \sum_{i,j=1}^{3} D_{ij}\psi_i\psi_j\, dS,$$

where D_{ij} are defined as in (28).

Acknowledgment. This work began when SG held a position at the California Institute of Technology.

REFERENCES

[1] D. Andelman, T. Kawakatsu, and K. Kawasaki, *Equilibrium shape of two-component unilamellar membranes and vesicles*, Europhys. Lett., 19 (1992), pp. 57–62.
[2] T. Baumgart, S. Das, W. W. Webb, and J. T. Jenkins, *Membrane elasticity in giant vesicles with fluid phase coexistence*, Biophys. J., 89 (2005), pp. 1067–1080.
[3] T. Baumgart, S. T. Hess, and W. W. Webb, *Imaging coexisting fluid domains in biomembrane models coupling curvature and line tension*, Nature, 425 (2003), pp. 821–824.
[4] D. Boal, *Mechanics of the Cell*, Cambridge University Press, Cambridge, UK, 2002.
[5] A. A. Boulbitch, *Equations of heterophase equilibrium of a biomembrane*, Arch. Appl. Mech., 69 (1999), pp. 83–93.
[6] S. Das, A. Tian, and T. Baumgart, *Mechanical stability of micropipet-aspirated giant vesicles with fluid phase coexistence*, J. Phys. Chem. B, 112 (2008), pp. 11625–11630.
[7] Q. Du, C. Liu, and X. Q. Wang, *A phase field approach in the numerical study of the elastic bending energy for vesicle membranes*, J. Comput. Phys., 198 (2004), pp. 450–468.
[8] C. M. Elliott and B. Stinner, *A surface phase field model for two-phase biological membranes*, SIAM J. Appl. Math., 70 (2010), pp. 2904–2928.
[9] D. M. Engelman, *Membranes are more mosaic than fluid*, Nature, 438 (2005), pp. 578–580.
[10] E. A. Evans and R. Skalak, *Mechanics and Thermodynamics of Biomembranes*, CRC Press, Boca Raton, FL, 1980.
[11] F. Feng and W. S. Klug, *Finite element modeling of lipid bilayer membranes*, J. Comput. Phys., 220 (2006), pp. 394–408.
[12] W. Helfrich, *Elastic properties of lipid bilayers - theory and possible experiments*, Z. Naturfors C, 28 (1973), pp. 693–703.
[13] D. E. Ingber, *Cellular mechanotransduction: Putting all the pieces together again*, Faseb. J., 20 (2006), pp. 811–827.
[14] D. E. Ingber, *Tensegrity-based mechanosensing from macro to micro*, Prog. Biophys. Mol. Bio., 97 (2008), pp. 163–179.
[15] F. Julicher and R. Lipowsky, *Domain-induced budding of vesicles*, Phys. Rev. Lett., 70 (1993), pp. 2964–2967.
[16] N. Kahya, D. Scherfeld, K. Bacia, B. Poolman, and P. Schwille, *Probing lipid mobility of raft-exhibiting model membranes by fluorescence correlation spectroscopy*, J. Biol. Chem., 278 (2003), pp. 28109–28115.
[17] F. B. Kalapesi, J. C. H. Tan, and M. T. Coroneo, *Stretch-activated channels: A minireview. Are stretch-activated channels an ocular barometer?*, Clin. Experiment. Ophthalmol., 33 (2005), pp. 210–217.
[18] A. Kloda, E. Petrov, G. R. Meyer, T. Nguyen, A. C. Hurst, L. Hool, and B. Martinac, *Mechanosensitive channel of large conductance*, Int. J. Biochem. Cell. B, 40 (2008), pp. 164–169.
[19] S. Leibler, *Curvature instability in membranes*, J. Phys. France, 47 (1986), pp. 507–516.
[20] J. S. Lowengrub, A. Raetz, and A. Voigt, *Phase-field modeling of the dynamics of multicomponent vesicles: Spinodal decomposition, coarsening, budding, and fission*, Phys. Rev. E (3), 79 (2009), 0311926.
[21] L. Ma and W. S. Klug, *Viscous regularization and r-adaptive remeshing for finite element analysis of lipid membrane mechanics*, J. Comput. Phys., 227 (2008), pp. 5816–5835.
[22] L. Miao, M. A. Lomholt, and J. Kleis, *Dynamics of shape fluctuations of quasi-spherical vesicles revisited*, Eur. Phys. J. E, 9 (2002), pp. 143–160.
[23] H. Naito and M. Okuda, *Preferred equilibrium structures of a smectic-a phase grown from an isotropic phase: Origin of focal conic domains*, Phys. Rev. E, 52 (1995), pp. 2095–2098.
[24] E. Perozo and D. C. Rees, *Structure and mechanism in prokaryotic mechanosensitive channels*, Curr. Opin. Struc. Biol., 13 (2003), pp. 432–442.
[25] R. Phillips, T. Ursell, P. Wiggins, and P. Sens, *Emerging roles for lipids in shaping membrane-protein function*, Nature, 459 (2009), pp. 379–385.
[26] U. Seifert, *Configurations of fluid membranes and vesicles*, Adv. in Phys., 46 (1997), pp. 13–137.
[27] U. Seifert, K. Berndl, and R. Lipowsky, *Shape transformations of vesicles: Phase diagram for spontaneous-curvature and bilayer-coupling models*, Phys. Rev. A, 44 (1991), pp. 1182–1202.

[28] P. Sens, L. Johannes, and P. Bassereau, *Biophysical approaches to protein-induced membrane deformations in trafficking*, Curr. Opin. Cell. Biol., 20 (2008), pp. 476–482.
[29] V. B. Shenoy and L. B. Freund, *Growth and shape stabillity of a biological membrane adhesion complex in the diffusion-mediated regime*, Proc. Natl. Acad. Sci. USA, 102 (2005), pp. 3213–3218.
[30] H. Sprong, P. van der Sluijs, and G. van Meer, *How proteins move lipids and lipids move proteins*, Nat. Rev. Mol. Cell. Bio., 2 (2001), pp. 504–513.
[31] D. Stamenovic and N. Wang, *Invited review: Engineering approaches to cytoskeletal mechanics*, J. Appl. Physiol., 89 (2000), pp. 2085–2090.
[32] J. J. Stoker, *Differential Geometry*, Wiley-Interscience, New York, 1969.
[33] S. I. Sukharev, W. J. Sigurdson, C. Kung, and F. Sachs, *Energetic and spatial parameters for gating of the bacterial large conductance mechanosensitive channel, mscl*, J. Gen. Physiol., 113 (1999), pp. 525–539.
[34] S. L. Veatch and S. L. Keller, *Separation of liquid phases in giant vesicles of ternary mixtures of phospholipids and cholesterol*, Biophys. J., 85 (2003), pp. 3074–3083.
[35] A. Veksler and N. S. Gov, *Phase transitions of the coupled membrane-cytoskeleton modify cellular shape*, Biophys. J., 93 (2007), pp. 3798–3810.
[36] M. R. Vist and J. H. Davis, *Phase-equilibria of cholesterol/dipalmitoylphosphatidylcholine mixtures: $\hat{2}h$ nuclear magnetic resonance and differential scanning calorimetry*, Biochemistry, 29 (1990), pp. 451–464.
[37] V. Vogel and M. Sheetz, *Local force and geometry sensing regulate cell functions*, Nat. Rev. Mol. Cell. Bio., 7 (2006), pp. 265–275.
[38] P. Wiggins and R. Phillips, *Membrane-protein interactions in mechanosensitive channels*, Biophys. J., 88 (2005), pp. 880–902.
[39] J. Yin, Y. Yin, and L. V. Cunjing, *General mathematical frame for open or closed biomembranes: Stability theory based on differential operators*, Appl. Math. Sci., 1 (2007), pp. 1439–1463.
[40] Y. Yin, *Integral theorems based on a new gradient operator derived from biomembranes (part* I*): Fundamentals*, Tsinghua Science & Technology, 10 (2005), pp. 372–375.
[41] Y. Yin, *Integral theorems based on a new gradient operator derived from biomembranes (part* II*): Applications*, Tsinghua Science & Technology, 10 (2005), pp. 376–380.
[42] Y. Yin, Y. Q. Chen, D. Ni, H. J. Shi, and Q. S. Fan, *Shape equations and curvature bifurcations induced by inhomogeneous rigidities in cell membranes*, J. Biomech., 38 (2005), pp. 1433–1440.
[43] Y. Yin, J. Yin, and J. Wu, *The second gradient operator and integral theorems for tensor fields on curved surfaces*, Appl. Math. Sci., 1 (2007), pp. 1465–1484.
[44] Y. J. Yin, J. Yin, and D. Ni, *General mathematical frame for open or closed biomembranes (part* I*): Equilibrium theory and geometrically constraint equation*, J. Math. Biol., 51 (2005), pp. 403–413.
[45] E. Zeidler, *Nonlinear Functional Analysis and Its Applications*, Springer-Verlag, New York, 1984.
[46] O. Y. Zhong-Can and W. Helfrich, *Bending energy of vesicle membranes: General expressions for the first, second, and third variation of the shape energy and applications to spheres and cylinders*, Phys. Rev. A, 39 (1989), pp. 5280–5288.
[47] C. Zhu, G. Bao, and N. Wang, *Cell mechanics: Mechanical response, cell adhesion, and molecular deformation*, Ann. Rev. Biomed. Eng., 2 (2000), pp. 189–226.